

# Alternating Copolymer of Double Four Ring Silicate and Dimethyl Silicone Monomer–PSS-1

Sam Smet,<sup>[a]</sup> Steven Vandenbrande,<sup>[b]</sup> Pieter Verlooy,<sup>[a]</sup> Stef Kerkhofs,<sup>[a]</sup> Eric Breynaert,<sup>[a]</sup> Christine E. A. Kirschhock,<sup>[a]</sup> Charlotte Martineau-Corcoss,<sup>[c]</sup> Francis Taulelle,<sup>[a, c]</sup> Veronique Van Speybroeck,<sup>[b]</sup> and Johan A. Martens<sup>\*,[a]</sup>

**Abstract:** A new copolymer consisting of double four ring (D4R) silicate units linked by dimethylsilicone monomer referred to as polyoligosiloxysilicone number one (PSS-1) was synthesized. The D4R building unit is provided by hexamethyleneimine cyclosilicate hydrate crystals, which were dehydrated and reacted with dichlorodimethylsilane. The local structure of D4R silicate units and dimethyl silicone monomers was revealed by multidimensional solid-state NMR, FTIR and modeling. On average, D4R silicate units have

6.8 silicone linkages. Evidence for preferential unidirectional growth and chain ordering within the PSS-1 copolymer was provided by STEM and TEM. The structure of PSS-1 copolymer consists of twisted columns of D4R silicate units with or without cross-linking. Both models are consistent with the spectroscopic, microscopic and physical properties. PSS-1 chains are predicted to be mechanically strong compared to silicones such as PDMS, yet more flexible than rigid silica materials such as zeolites.

## Introduction

Building in space with supramolecular building blocks is an imaginative approach to material design.<sup>[1–12]</sup> In the world of silicon-based materials the octameric cyclosilicate oligomer  $[\text{Si}_8\text{O}_{12}]$ , also known as double four ring (D4R), is such an imaginative building block. Its symmetrical cubic core and the possibility to attach chemical groups on the eight corners make the D4R silicate unit a versatile platform for synthesis of a whole range of materials.<sup>[2,13–16]</sup> D4R silicate units are building blocks of inorganic and organic–inorganic hybrid materials including zeolites, cyclosilicates, cyclosilicate hydrates, polyhedral oligomeric silsesquioxanes (POSS), and spherosilicates. In these materials, D4R silicate units are engaged either in covalent bonding, electrostatic bonding or hydrogen bonding. The D4R building unit is a very common secondary building unit of zeolite frameworks. It occurs in 33 of the 232 listed zeolite framework types.<sup>[17]</sup> The popular zeolite A (LTA topology) for example, is made entirely out of D4R units. Cyclosilicates are crystal-

line materials with negatively charged rings of  $\text{SiO}_4$  tetrahedra. In cyclosilicate (CyS) crystals the charge of the D4R unit with formula  $[\text{Si}_8\text{O}_{12}][\text{O}^-]_n[\text{OH}]_{8-n}$  is compensated by inorganic or organic cations. In the subgroup of cyclosilicate hydrates (CySH) the D4R units are engaged in a hydrogen-bonded network involving water molecules and amines.<sup>[14,18–21]</sup> Cyclosilicate hydrates are precursor materials for synthesis of spherosilicates.<sup>[4,7,8,14–16,22–24]</sup>

Spherosilicates and the related octameric polyhedral oligomeric silsesquioxane (POSS) family have the D4R silicate unit as core and functional groups attached to its eight corners. These functional groups are siloxy groups ( $\text{OSiR}_3$ ) in spherosilicates and hydrogen, alkyl or alkoxy groups in POSS.<sup>[13,14]</sup> The combination of a chemically inert D4R silicate core with endlessly tunable functional groups renders these compounds highly useful as organic–inorganic hybrid materials.<sup>[2–4,25–28]</sup> Advances in spherosilicate and POSS chemistry in recent years enabled the synthesis of sophisticated D4R-based polymer materials.<sup>[2]</sup> They have been assembled in organolithic macromolecular materials,<sup>[29]</sup> dendrimers<sup>[8]</sup> and marshmallow-like mesoporous to macroporous gels.<sup>[7,30–34]</sup>

The combination of D4R silicate units with silicone leads to unique materials combining properties of both silica and silicone. Synthesis of such hybrids is not trivial however. Reaction of D4R cyclosilicate hydrate with multifunctional silanes such as dichlorodimethylsilane results in a randomly cross-linked network of D4R units and silicone bridges of variable length.<sup>[11]</sup> The crystal water present in the CySH precursor crystals causes hydrolysis and unselective reaction.<sup>[4,15,23,35–38]</sup>

Previously we reported the synthesis of CySH material with formula  $[\text{C}_6\text{H}_{14}\text{N}]_4[\text{Si}_8\text{O}_{16}(\text{OH})_4] \cdot 12\text{H}_2\text{O}$  that can be dehydrated without degradation of the D4R units.<sup>[21]</sup> In this work we used this anhydrous precursor material for synthesizing silicone–silicate alternating copolymers.

[a] S. Smet, Dr. P. Verlooy, Dr. S. Kerkhofs, Dr. E. Breynaert, Prof. Dr. C. E. A. Kirschhock, Prof. Dr. F. Taulelle, Prof. Dr. J. A. Martens  
Centre for Surface Chemistry and Catalysis  
KU Leuven  
Celestijnenlaan 200f–2461; 3001 Leuven (Belgium)  
E-mail: johan.martens@kuleuven.be

[b] S. Vandenbrande, Prof. Dr. V. Van Speybroeck  
Centre for Molecular Modeling  
Ghent University  
Technologiepark 903, 9052 Zwijnaarde (Belgium)

[c] Dr. C. Martineau-Corcoss, Prof. Dr. F. Taulelle  
Institut Lavoisier de Versailles  
University of Versailles  
Versailles (France)

Supporting information for this article can be found under:  
<https://doi.org/10.1002/chem.201701237>.

## Results and Discussion

### PSS-1 synthesis

The targeted copolymer consists of D4R units, the corners of which are interlinked with dimethylsilicone monomer units (Figure 1 right). Hexamethylenimine cyclosilicate hydrate (HMI-CySH) served as source of D4R silicate units.

HMI-CySH was crystallized according to a previously reported method.<sup>[21]</sup> The powder was isolated from the aqueous synthesis medium, washed with water and dried to obtain anhydrous crystals (HMI-CyS). In the structure of HMI-CySH the D4R silicate units adopt a columnar arrangement by hydrogen bonding with water and HMI molecules (Figure 1 left).<sup>[21]</sup> In the dehydrated structure (HMI-CyS) the silanols of D4R are hydrogen bonded with HMI molecules (Figure 1 middle).

The copolymerization reaction was performed by reacting HMI-CyS powder with dichlorodimethylsilane (DCDMS). A white precipitate was recovered consisting of PSS-1 copolymer and HMI chloride salt crystals. HMI chloride was removed by a washing procedure.

### NMR

Chemical shifts of <sup>29</sup>Si magic-angle spinning (MAS) NMR spectra were externally referred to tetramethylsilane. The <sup>29</sup>Si MAS NMR spectra of HMI-CySH and HMI-CyS show one resonance at -100 ppm, as-

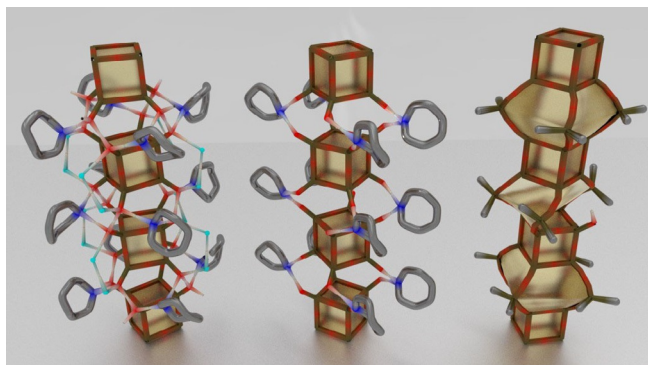


**Figure 1.** Representation of the columnar stacking of D4R units in the structure of HMI-CySH (left), HMI-CyS (middle)<sup>[21]</sup> and a hypothetical model of PSS-1 copolymer.

signed to the silicon atoms of D4R, in agreement with previous work (Figure 2A in grey).<sup>[21]</sup> In <sup>29</sup>Si NMR literature Si atoms are denoted with a code consisting of a letter followed by a number. The letter symbolizes the amount of O atoms directly bound to the Si atom (M, D, T, or Q for the respective cases of 1, 2, 3, or 4 O atoms) and the number reflects the amount

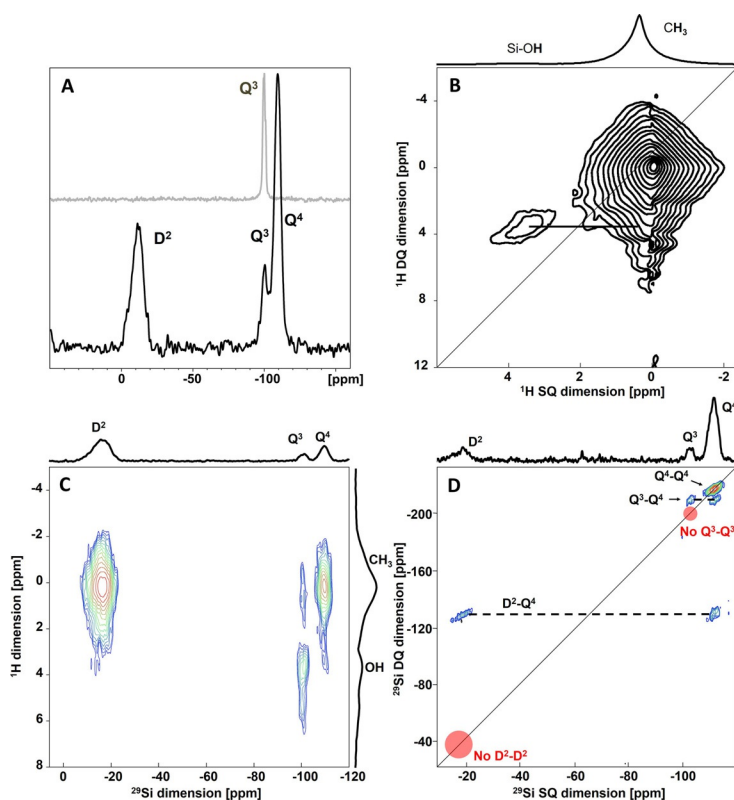


**Figure 2.** A) <sup>29</sup>Si NMR spectra of HMI-CyS (grey) and PSS-1 (black); B) <sup>1</sup>H-<sup>29</sup>Si SODQ MAS NMR spectrum of PSS-1; C) <sup>1</sup>H-<sup>29</sup>Si HETCOR MAS NMR spectrum of PSS-1 showing that the D<sup>2</sup> and Q<sup>4</sup> Si species are in close proximity to the methyl-protons while Q<sup>3</sup> is more related with the silanol-protons; D) <sup>29</sup>Si-<sup>29</sup>Si SODQ NMR spectrum of PSS-1 showing the connection between D<sup>2</sup>-Q<sup>4</sup>, Q<sup>3</sup>-Q<sup>4</sup> and Q<sup>4</sup>-Q<sup>4</sup> and the absence of Q<sup>3</sup>-Q<sup>3</sup> and D<sup>2</sup>-D<sup>2</sup>.

of those O atoms who in turn are bound to a second Si atom. For example the Si atoms present in HMI-CySH or HMI-CyS, containing three siloxane linkages and one silanol, are denoted with the Q<sup>3</sup> symbol.<sup>[39,40]</sup> The targeted polymer is expected to show two <sup>29</sup>Si MAS NMR signals: one due to the Si atoms with four siloxane bonds at the corners of D4R silicate units denoted as Q<sup>4</sup> and one due to dimethylsilicone linkers denoted as D<sup>2</sup>. The <sup>29</sup>Si MAS NMR spectrum of PSS-1 shows three main signals at -16, -100, and -110 ppm, respectively (Figure 2A in black). Through deconvolution of the signal at -16 ppm, a fourth signal at -10 ppm could be observed (see Supporting Information Figure 1). The two signals dominating the <sup>29</sup>Si MAS NMR spectrum of PSS-1 at -16 and -110 ppm are assigned to the expected D<sup>2</sup> and Q<sup>4</sup>, respectively which is in agreement with literature.<sup>[39,40]</sup>

The presence of additional signals reveals that some D4R Si atoms are lacking a linker (Q<sup>3</sup> signal at -100 ppm) and that side reactions of dimethyldichlorosilane occurred (signal at -10 ppm). Quantification of the Q<sup>3</sup> and Q<sup>4</sup> signals reveals 84.7% (or about 7 out of 8) of the D4R Si atoms to have a silicone linkage. Based on literature, the <sup>29</sup>Si MAS NMR signal at -10 ppm could be due to dimethylsilicone three-ring, denoted D<sup>2Δ</sup><sup>[39]</sup> or dimethylsilane bonded to only one D4R and carrying a hydroxyl group, that is, a D<sup>1</sup> silicon species.<sup>[39]</sup> It represents 5.4% of the <sup>29</sup>Si MAS NMR signal. The Q<sup>4</sup>/D<sup>2</sup> signal ratio (= 1.96) is close to 2, suggesting few silicone bridges to be defec-

tive. Dangling  $D^1$  groups on D4R corners are thus unlikely to contribute substantially to the  $-10$  ppm signal. Assignment of the signal to  $D^{2A}$  molecules not being part of the polymer is more likely.

The  $^{13}\text{C}$  MAS NMR spectrum of PSS-1 showed a resonance around 0 ppm assigned to methyl groups (Supporting Information Figure 2). Absence of  $^{13}\text{C}$  MAS NMR signals due to HMI confirmed it was successfully removed from the final product.  $^1\text{H}$  MAS NMR revealed the occurrence of three different H environments: silanols with a chemical shift of 3.6 ppm and two signals around 0 ppm due to methyl groups (Supporting Information Figure 3).

Two-dimensional NMR provided deeper insight in the chemistry of PSS-1. The  $^1\text{H}-^1\text{H}$  MAS single-quantum double-quantum (SQDQ) NMR spectrum (Figure 2B) displays strong correlation between protons of different methyl groups and between protons of methyl groups and silanol protons, which reveals close proximity. Silanol protons among themselves do not produce a correlation signal and are thus too far apart for transferring magnetization. This observation favors the assignment of  $Q^3$  Si signals in the  $^{29}\text{Si}$  MAS NMR spectrum (Figure 2A) to unreacted D4R corners rather than broken bonds of D4R silicate units, which would be in close proximity. Using a  $^1\text{H}-^{29}\text{Si}$  MAS heteronuclear correlation (HETCOR) experiment (Figure 2C), spatial correlations between protons and Si atoms can be probed. The spectrum reveals that both  $D^2$  and  $Q^4$  Si atoms are in close proximity to methyl protons, which is expected when D4R is systematically linked with dimethylsilicone monomer.  $Q^3$  Si lacking silicon linker are strongly correlated to the protons of the silanols as expected.  $Q^3$  Si atoms of D4R show weak correlation with methyl protons, consistent with the idealized structure with D4R silicate units spaced by dimethylsilicone monomers. The absence of a correlation signal between the protons of the silanols and the Si species at  $-10$  ppm confirms the assignment of the latter signal to an unrelated molecule such as  $D^{2A}$  rather than  $D^1$  of a defective silane bridge terminated by a hydroxyl group. The presence of cyclic dimethylsilicone trimer explains the sharp  $^1\text{H}$  MAS NMR signal around 0 ppm originating from the methyl groups on these highly mobile Si-species (Supporting Information Figure 3). Finally, the  $^{29}\text{Si}-^{29}\text{Si}$  MAS SQDQ NMR spectrum of PSS-1 (Figure 4D) clearly shows the connection between  $Q^4$ 's representing adjacent silicon corners of D4R silicate units, between  $Q^3$  and  $Q^4$  within the same D4R unit and between  $D^2$  and  $Q^4$  due to the attachment of a silicone linker to a corner of a D4R silicate unit. The absence of correlation signal between  $D^2$  species confirms the interlinking of D4R with dimethylsilicone monomer rather than oligomer. The  $D^{2A}$  species also does not appear to generate a correlation signal between  $D^2$  species. Most likely this is due to the low concentration of this molecule (only 5.4% of the total Si content). Finally, the absence of correlation between  $Q^3$ 's confirms that unreacted silanols on different D4R silicate units are far apart, precluding the presence of adjacent silanols on a same D4R and hydrogen-bridged silanols of different D4R silicate units.

## ATR-FTIR

FTIR spectra of PSS-1 and HMI-CyS are shown in Figure 3 and compared with spectra computed on two clusters. The first cluster ( $T_8$ ) represents a D4R silicate unit with formula  $\text{Si}_8\text{O}_{12}(\text{OH})_8$ , while for the second cluster ( $T_8(D_2)$ ) one of the hydroxyls was replaced by an  $\text{OSi}(\text{CH}_3)_2[\text{Si}(\text{OH})_3]$  silicone linker (Supporting Information Figure 4) to also simulate the typical frequencies associated with the linker connection.

The simulated FTIR spectra were calculated with DFT using Gaussian.<sup>[41]</sup> The B3LYP<sup>[42]</sup> functional with D3BJ<sup>[43]</sup> dispersion corrections was used together with a 6-311+G(d,p)<sup>[44,45]</sup> basis

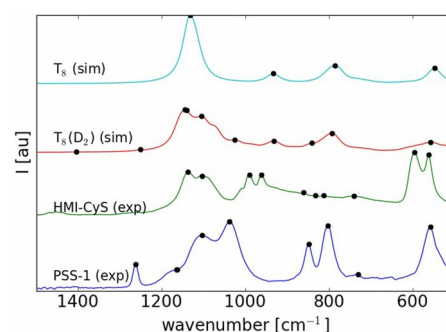


**Figure 3.** A comparison between the theoretical IR spectra of  $T_8$  and  $T_8(D_2)$  and the experimental IR spectra of HMI-CyS and PSS-1 particles in the lower wavenumber region (the entire IR spectral range can be found in Supporting Information Figure 5).

set. Because of the systematic overestimation of the vibrational frequencies, a factor of 0.96 was applied to all simulated frequencies as suggested in literature.<sup>[46]</sup> There is a good agreement in signal band position between the experimental and simulated spectra (see Supporting Information Figures 5–7). The resonance bands originating from vibrations of the cube at  $1162\text{ cm}^{-1}$  (asymmetric Si-O-Si stretch-shoulder),  $1104\text{ cm}^{-1}$  (asymmetric Si-O-Si stretch), and  $557\text{ cm}^{-1}$  (Si-O-Si bending) are present in the experimental IR spectra from both HMI-CyS and PSS-1 particles. This confirms PSS-1 to be composed of D4R silicate units. Vibrations of the dimethyl silicone linkers at  $1261\text{ cm}^{-1}$  ( $\text{CH}_3$  umbrella),  $1038\text{ cm}^{-1}$  (asymmetric Si-O-Si stretch),  $848\text{ cm}^{-1}$  ( $\text{CH}_3$  rocking) and  $731\text{ cm}^{-1}$  (symmetric Si-O-Si stretch) are present in the IR spectrum of PSS-1 and not in the HMI-CyS precursor, as expected. Note that the intensity of these vibrational bands is underestimated in the simulations because of the model possessing only one silicone linker. The resonance band originating from the terminal Si-O stretch of a corner of the D4R unit at  $930\text{ cm}^{-1}$  is clearly present in the IR spectrum from the HMI-CyS crystals. The weak intensity of this resonance band in the IR spectrum of the PSS-1 confirms that a minority of the D4R corners are lacking a silicone linker.

## HR-TEM/STEM

Scanning transmission electron microscopy (STEM) images of PSS-1 showed the presence of linear particles of around 200–300 nm long and up to around 40 nm wide. Some isolated wires with a width of around 1 nm were also observed (Figure 4A). The diameter of the thinnest wires according to STEM corresponds to the size of one D4R silicate unit, measuring approximately 0.9 nm. The elementary wire seems to consist of a single chain of D4R units linked with dimethyl silicone groups. Solubilization of PSS-1 in different solvents to isolate more wires was attempted (THF and chloroform). The presence of dissolved polymer was investigated using liquid  $^{29}\text{Si}$  single-pulse NMR. Despite choosing measuring conditions sufficient to detect low concentrations in solution,<sup>[47]</sup> no  $^{29}\text{Si}$  signal was recorded, meaning that the solubility was below the NMR detection limit.

High resolution transmission electron microscopy (HR-TEM) images of the PSS-1 particles (Figure 4B) reveal some internal order in one direction. The parent HMI-CyS crystals investigated earlier display similar spacing in their TEM pattern.<sup>[21]</sup> Si atoms present in PSS-1 are likely to scatter more strongly in TEM compared to C, O, and H atoms. The white parallel lines observed are assigned to the presence of linear arrangements

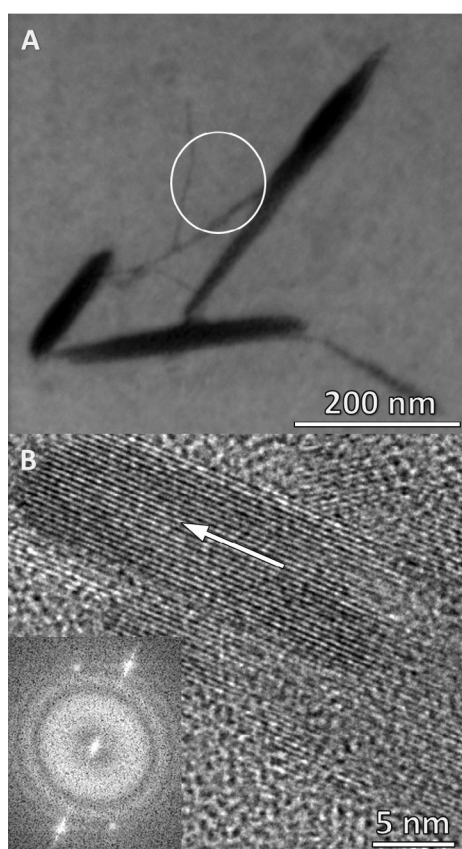


**Figure 4.** A) a STEM image of PSS-1 taken with an electron beam of 16.0 keV. An individual chain with a thickness of approximately 1 nm is visible (inside the white circle). B) a high-resolution transmission electron microscopy image of PSS-1. The direction of the chains is indicated by a white arrow. The fast Fourier transformation of the image is included in lower left corner.

of Si atoms. The distances between these lines, determined by fast Fourier transformation, are in the range of 0.29–0.32 nm. This distance coincides with a typical distance of Si-O-Si bonds (e.g. in the D4R units).

The X-ray diffraction pattern of PSS-1 was recorded to further investigate long range ordering within the material. The X-ray diffraction pattern was unexpectedly broad despite the observed periodicity in TEM, and the presence of structures of around 40 by 200 nm (Figure 4). This would signify that the larger structures do not exhibit high periodicity throughout their volume.

The structure of PSS-1 can be interpreted as being composed of chains of alternating D4R units and dimethylsilicone monomers (Figure 1 right) with every D4R unit possessing either 1 or 2 unreacted corners (Q<sup>3</sup> species) ending in hydroxyl groups. The low solubility can be reconciled with the proposed structure provided strong van der Waals interaction prevents dissolution in organic solvent<sup>[48,49]</sup> (Figure 5 left), or if chains are cross-linked (Figure 5 right). Such cross linking would not be detected by the solid state NMR methods used in this manuscript.

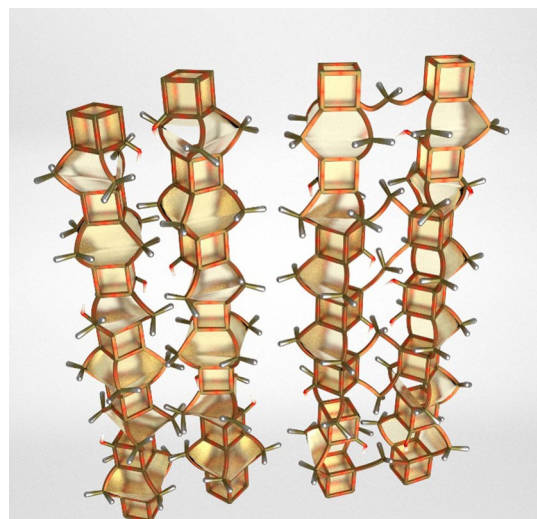


**Figure 5.** Linking modes of D4R-dimethylsilicone copolymer chains based on van der Waals interaction (left) and random cross-linking (right). Deformation due to flexibility of the linkers is ignored.

## PSS-1 Model

Physicochemical characterization in previous sections suggest PSS-1 to be essentially composed of copolymer chains of D4R and dimethyl silicone monomer. PSS-1 is, to the best of our knowledge, the first material wherein oligomeric cyclosilicates are connected by monomeric silicone linkers in an alternating fashion.

According to the Q<sup>4</sup> content determined by  $^{29}\text{Si}$  MAS NMR and the Q<sup>3</sup> and Q<sup>4</sup> content (Figure 2A), each D4R silicate unit is lacking about one silicone linkage. The chemical structure of PSS-1 was investigated using a variety of theoretical models. First the influence of defects was investigated by studying the breaking of a linker from its D4R silicate unit (Figure 6). This

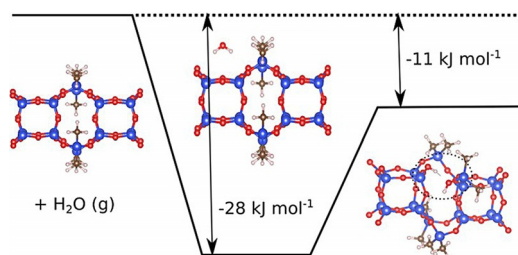


**Figure 6.** Difference in electronic energy between D4R silicate units linked by a dimethylsilicone bridge (left) and the reaction with water to form a D<sup>1</sup> defect (right). Si atoms in blue, oxygen atoms in red, C atoms in brown and H atoms in white.

breaking of the linker is modeled through the incorporation of one water molecule (for each D4R silicate unit) in order to properly terminate the structure, creating a D<sup>1</sup> silicon atom at one corner. The (free) energies of the one-dimensional periodic structures are calculated with DFT (using VASP<sup>[50]</sup> with the PBE-D3BJ<sup>[51]</sup> functional). The model revealed that the creation of such a D<sup>1</sup> defect is certainly possible given the small energy difference between the fully connected structure and the structure where one linker defect has been introduced.

Next, the energy of two potential structures was computed: one with missing linkers but little twisting of the chain and one with missing linkers and severe twisting of the chain. Calculations (using Gaussian at the B3LYP-D3BJ/6-31+G(d,p) [LanL2DZ for Si atoms] level-of-theory) show that the severely twisted chain is favored energetically compared to models with D4R with almost the same orientation (14° angle of rotation), but not entropically. At 300 K however the twisted configuration is still the most stable one (Figure 7). The difference in free energy is small, indicating that both structures are likely to occur. The optimal twist angle is about 44°. The relative rotation of D4Rs can explain the missing silicone linkages. A relative rotation by 44° makes one of the four corners of a D4R silicate unit unavailable for linking. Such bonding mode avoids close proximity of unlinked D4R corners, as concluded from the <sup>1</sup>H-<sup>1</sup>H SQDQ NMR (Figure 2B) and <sup>29</sup>Si-<sup>29</sup>Si SQDQ NMR spectra (Figure 2D).

The parent HMI-CySH material exhibits the same type of D4R twisting along the axis of the column in an alternating fashion.<sup>[21]</sup> Relative rotation by around 21° between two adjacent D4R units generates the shortest distance of ±2.5 Å between the silanol oxygen atoms of the D4R corners. To bridge

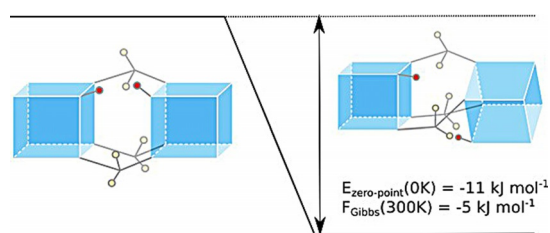


**Figure 7.** Schematic representation of the energy difference between a structure of PSS-1 with missing linkers but no twisting of the chain (left) and one with missing linkers and twisting of the chain (right).

two oxygen atoms by the insertion of a silicon atom, typically a distance between 2 and 3 Å is required depending on the angle of the bonds at the silicon atom. For a perfect tetrahedral conformation and a Si-O bond length of 1.63 Å (which is the typical bond length in polydimethylsilicone) this distance would be 2.65 Å. The short distance between two silanols of two adjacent D4R units in the HMI-CyS material is ideal for making such a connection. The similarity of D4R columnar structures of the parent HMI-CyS and PSS-1 invites for a speculation on the polymerization mechanism. The relative rotation may explain the systematic absence of linker. During the bridging reaction of D4Rs of HMI-CyS with dichlorodimethylsilane, HMI molecules need to be displaced. Dichlorodimethylsilane probably first reacts with one of the two D4R units, displaces the present HMI molecule and only then reacts with the second D4R unit. During this displacement the D4R units can gain in mobility which in turn allows the dangling chlorosilyl to react not with the previously nearest silanol of the adjacent D4R unit, but with the silanol group next to it. Once this has happened those two D4R units are connected by three dimethyl silicone monomers instead of four.

### Physical and chemical properties

Some physical properties of PSS-1 were derived from the theoretical model. Of particular interest is Young's modulus which reveals how much force has to be applied to the material to deform it. Young's modulus was computed in the direction of the periodic dimension assuming that the copolymer is periodic along the *x*-axis (Supplementary 8). The first computation assumed complete linkage of D4Rs with dimethyl silicone. Young's modulus in the *x* direction  $Y_{xx}$  is defined as:

$$Y_{xx} = \frac{\Delta E}{A_{yz} \Delta a} \cdot \frac{a_0}{\Delta a}$$

where  $A_{yz}$  is the surface orthogonal to the *x* direction and *a* is the cell parameter in the *x* direction. The Young modulus  $Y_{xx}$  amounted to 14.5 GPa for an optimal cell length  $a = 7.63$  Å. The same procedure was applied to a PSS-1 chain where one out of four linkers was broken. This leads to a dangling O atom and Si atom, which are terminated with an H atom and an OH atom, respectively. This leads to a Young's modulus less than half the value for the complete PSS-1,  $Y_{zz} = 7.3$  GPa. The optimal cell length is also smaller than in the previous case,  $a = 7.48$  Å. Note that according to NMR only 1 out of 8 linkers are suspected to be missing, so the Young's modulus is expected to be in between 6.4 GPa and 14.5 GPa. These values are in between those of rigid materials like zeolites (with bulk moduli of 15 GPa to at least 100 GPa)<sup>[52,53]</sup> and common silicones (Young moduli of only 10–100 MPa)<sup>[54]</sup> or other common polymers (e.g. ABS, PVC, nylon, PTFE, polystyrene) with Young moduli up to 4.5 GPa.<sup>[55]</sup> A common practice to increase the Young moduli of polymers is by adding rigid additives (e.g. glass fibers) although this results rarely in Young moduli exceeding 10 GPa.<sup>[55]</sup>

A common feature between PSS-1 and silicones is the combined presence of organic groups and a flexible inorganic part, which gives silicones their unique properties (electrical insulation, biocompatibility, weathering resistance).<sup>[56]</sup> In PSS-1 however these monomers are combined with the more rigid D4R units, increasing the silicon to carbon ratio to 1.5 (0.5 in the case of silicones).

POSS are usually synthesized by the condensation reaction of silanes with formula  $\text{SiX}_3\text{R}$ , with X being a leaving group and R being the desired group of the final POSS. A nearly unavoidable side-product are silsesquioxanes with a ladder type repeating unit. First reported by Brown et al. (1960)<sup>[57]</sup> these mostly linear organic/inorganic hybrid polymers are structurally similar to PSS-1. The essential difference is the higher silicon content of PSS-1 because of the D4R cages.

Spherosilicates have been linked together to form organic/inorganic hybrid amorphous gels.<sup>[1,7,9]</sup> Chemically those materials are similar to PSS-1. The D4R units are however linked randomly by silicone chains of variable length resulting in a three dimensional gel-like structure. In PSS-1 the D4R units are interlinked by dimethylsilicone monomers in columnar structures.

The thermal stability of the organic groups on PSS-1 ( $=\text{CH}_3$  groups) was compared with the well-known polydimethylsiloxane (PDMS). Thermogravimetric analysis in oxygen atmosphere revealed the oxidation of methyl groups to start at 460 °C, whereas on PDMS it occurs at 400 °C. Under nitrogen atmosphere the methyl groups of PSS-1 are stable to at least 750 °C whereas on PDMS the degradation process already starts at 500 °C. PSS-1 thus appears to be far more thermally stable compared to the related PDMS, both in oxidative and inert atmosphere. (Supporting Information Figures 9, 10). Related MQ copolymers, which are networks of  $\text{Q}^4$  Si species typically end-capped by trimethylsiloxy groups ( $\text{M}^1$  species), have shown a similar increase of the thermal stability of the organic groups by increasing the  $\text{Q}^4$  content of the copolymer.<sup>[58–60]</sup> Material with high  $\text{Q}^4$  content shows elimination of methyl groups below 700 °C in similar conditions where PSS-1 withstands at least 750 °C.<sup>[58]</sup> Other D4R containing polymers with organic groups seldom demonstrate a thermal stability of these groups above 700 °C.<sup>[61,62]</sup>

The synthesis method of PSS-1, in which building blocks inside an already ordered structure are interlinked together by the insertion of reactive linkers, is similar to the proven method of synthesizing new materials by connecting the layers of layered silica or layered zeolites.<sup>[63]</sup> A strong point of this methodology is the possibility to rearrange these two-dimensional building blocks before interconnecting them (e.g. expanding or shrinking the interlayer, delamination or recombination of the layers). In the case of expanding the interlayer, instead of connecting the layers directly, typically an organosilylating agent (usually containing two methyl groups and two leaving groups (chloro-, ethoxy-, methoxy-)) is used to link them together. Changing the used building block, being either the layers and/or the linking agent, are other relatively easy methods for designing new materials.

By decreasing the dimensionality of the rather large two-dimensional layers to the zero-dimensional D4R units, the versa-

tility of this synthesis method has been dramatically increased even further. PSS-1 is thus probably the first of a whole range of new materials synthesized using this building block based method. Another example of a building block based material family, namely the metal organic frameworks (MOFs), based on a combination of metallic clusters and organic linkers, clearly shows the strength and the theoretical potential of such methods.

## Conclusion

Polyoligosiloxysilicone number-1 (PSS-1) is a new alternating copolymer wherein D4R units are connected by dimethylsilicone monomers. The chemical structure was derived from one and two dimensional solid-state NMR investigations, FTIR and computational modeling. Additionally, STEM, and TEM provided evidence of preferential growth in one direction. A theoretical model of the chains of PSS-1 material is proposed, characterized by systematic twisting of the D4R units along the longitudinal axis made possible by the absence of one linker per D4R. In this model the cyclosilicate–silicone hybrid adopts the columnar arrangement of D4R units of the parent hexamethyleneimine cyclosilicate (HMI–CyS) in which the D4R arrangement is imposed by hydrogen bonding. The twisted D4R configuration is retained after transformation to PSS-1 through annealing with dichlorodimethylsilane. These structures could be held together by strong van der Waals forces or cross linking. PSS-1 likely is the first example of a range of new silicate–silicone hybrid materials where cyclosilicate oligomers are tightly interlinked by silicone linkers. The enhanced silicon content of PSS-1 compared to typical silicones improves mechanical strength and thermal stability. The synthesis of PSS-1 in which zero dimensional building blocks (DR4) in an already pre-organized weakly bonded structure (HMI–CyS) are permanently fixed by insertion of reactive linkers is a new approach of silicone materials design.

## Experimental Section

### Synthesis HMI crystals<sup>[21]</sup>

HMI–CySH crystals were synthesized by adding tetraethylorthosilicate (TEOS) (5 mL, Acros 98%) under vigorous stirring to an aqueous (15 mL, MilliQ water) solution of hexamethyleneimine (HMI) (5 mL Acros 99%) at room temperature. The solution was continuously stirred for seven days until crystals formed. The final crystals were recovered from the solution by filtration. After drying at room temperature the HMI–CySH crystals transformed into water-free HMI–CyS crystals.

### PSS-1 synthesis

2 g of HMI–CyS crystals were dried under vacuum (<1 mbar) for 48 hours in a two-neck 1 L round bottom flask. 50 mL of tetrahydrofuran (THF, Sigma Aldrich  $\geq 99.9\%$ ) was mixed with 50 mL of dichlorodimethylsilane (DCDMS, Acros 99%). This mixture was distilled until 60 mL of liquid was obtained of which 20 mL was added to the dried HMI–CyS crystals. The formed suspension was stirred for 5 minutes and subsequently filtered and dried under

vacuum over a glass filter (vitapore 4, P16). Part of the obtained particles were washed with a mixture of equal volumes of distilled water, acetone (Chem Lab 99.5%) and toluene (VWR 99.8%) and rinsed with distilled water to remove any remaining organics.

### Characterization

Scanning transmission electron microscopy (STEM) images were taken on a Nova NanoSem 450 with an electron beam energy of 16 kV. To obtain a relatively good dispersion, the particles were suspended in THF and one drop of this suspension was dripped on the carbon lacey grid. High resolution transmission electron microscopy (TEM) images were obtained using a Philips CM200 FEG (Philips, Eindhoven, The Netherlands) operated at 200 kV. Before examination, the particles were dispersed in an acetone/water mixture and deposited on a copper grid.

ATR-FTIR spectra were measured on a Bruker Alpha Platinum ATR spectrometer with a single reflection diamond crystal and a room temperature DTGS detector. The absorbance in the infrared spectrum from 4000  $\text{cm}^{-1}$  to 375  $\text{cm}^{-1}$  was calculated from 128 scans with a resolution of 4  $\text{cm}^{-1}$ .

All solid-state NMR samples were packed in a 4 mm zirconia rotor. Tetramethylsilane was used as an external chemical shift reference for  $^1\text{H}$ ,  $^{13}\text{C}$ , and  $^{29}\text{Si}$ . All measurements were performed with the natural abundance of the measured element.

All MAS NMR spectra of PSS-1 were recorded on a Bruker Avance 500 spectrometer at a resonance frequency of 500.1 MHz for  $^1\text{H}$ , 125.7 MHz for  $^{13}\text{C}$ , and 99.3 MHz for  $^{29}\text{Si}$ . The samples were spun at 10 kHz for the 1D measurements and the  $^1\text{H}$ - $^1\text{H}$  2D measurement and at 5.5 kHz for the other 2D measurements. For the  $^1\text{H}$  MAS NMR spectrum 16 scans were recorded with a recycle delay of 3 s and a  $90^\circ$  pulse of 3  $\mu\text{s}$ . The  $^1\text{H} \rightarrow ^{13}\text{C}$  cross-polarization (CP) MAS NMR spectrum was recorded using a 3.5 ms contact time, 4 s recycle delay and  $^1\text{H}$  SPINAL-64 decoupling. 128 transients were accumulated. For the quantitative single-pulse  $^{29}\text{Si}$  MAS NMR spectrum, 448 scans were recorded with a recycle delay of 500 s and a  $90^\circ$  pulse of 3.75  $\mu\text{s}$ . The  $^1\text{H}$ - $^1\text{H}$  SQDQ MAS NMR spectrum used the back-to back (BABA) sequence with recoupling time of 0.4 ms. 50  $t_1$  slices with 32 transients each were recorded with a recycle delay of 1 s. For the  $^1\text{H}$ - $^{29}\text{Si}$  HETCOR MAS NMR spectrum, the contact time was set to 9 ms, 50  $t_1$  slices with 64 transients each were recorded, with recycle delay of 1 s. For the  $^{29}\text{Si}$ - $^{29}\text{Si}$  SQDQ MAS NMR spectrum 140  $t_1$  slices with 104 transients each with a recycle delay of 3 s were recorded. The  $^{29}\text{Si}$  magnetization was prepared using a CP from  $^1\text{H}$  of 8 ms. All two-dimensional NMR spectra were recorded using the States procedure to obtain phase sensitive spectra.

Dissolution experiments were performed by mixing 50 mg of PSS-1 powder with 3 mL of tetrahydrofuran (Sigma Aldrich  $\geq 99.9\%$ ) or chloroform (Acros 99+%) and sonicating the mixtures for 1 h. A couple of drops of deuterated tetrahydrofuran or chloroform were added prior to measuring to ensure a decent lock signal. Solution  $^{29}\text{Si}$  NMR spectra were recorded on an Avance II 600 MHz spectrometer. Up to 256 scans were recorded using a  $^{29}\text{Si}$   $90^\circ$  pulse of 13.7  $\mu\text{s}$  and a delay time of 60 s. Thermogravimetric analyses were performed on a TGA-Q500 TA. Samples were heated at  $10^\circ\text{Cmin}^{-1}$  from room temperature to  $750^\circ\text{C}$  under a flow of  $\text{N}_2$  or  $\text{O}_2$  gas.

Colorless Dow Corning DC 976 High-Vacuum Silicon Grease was used as reference polydimethylsiloxane sample.

## Computational modelling

### Cluster calculations

All cluster calculations were performed using Gaussian 09 Revision D.01 with tight SCF convergence using XQC and an ultrafine grid for numerical integrals.

### Periodic calculations

All periodic calculations were performed using VASP 5.3.3. The plane wave cut-off was 600 eV, a Monkhorst-Pack  $5 \times 1 \times 1$  k-point grid was used. The SCF was considered to be converged if the energy change was smaller than  $10^{-8}$  eV, structural optimizations were considered converged if the energy change was smaller than  $10^{-6}$  eV. A  $30 \times 30 \text{ \AA}$  cell in the non-periodic dimensions was used to simulate the one-dimensional structures.

To determine Young's modulus  $Y_{\text{xxx}}$  a relaxed scan over the a cell parameter for the isolated PSS-1 chain was performed and fitted with a parabola to the obtained energy curve. Young's modulus can then be obtained analytically from this fit. The surface  $A_{yz}$  was calculated to be  $10.8 \times 10.8 \text{ \AA} = 116 \text{ \AA}^2$  by studying the stacking of the one dimensional structures. (Supporting Information Figure 11).

## Acknowledgements

We acknowledge the Flemish government for long-term structural funding (Methusalem), the Research Foundation–Flanders (FWO), the Research Board of Ghent University (BOF), and BELSPO in the frame of IAP/7/05 for financial support. Computational resources and services were provided by Ghent University (Stevin Supercomputer Infrastructure). The acquisition of HR-TEM and NMR instrumentation was supported by the Flemish Hercules Foundation (HER/08/25 and AKUL/1321).

## Conflict of interest

The authors declare no conflict of interest.

**Keywords:** multidimensional NMR • oligomers • polyoligosiloxysilicone • polymers • silicon

- [1] I. Hasegawa, *J. Sol-Gel Sci. Technol.* **1995**, *5*, 93–100.
- [2] J. Xu, Q. Ye, H. Zhou, *Chem. Asian J.* **2016**, *11*, 1322–1337.
- [3] T. Engel, G. Kickelbick, *Eur. J. Inorg. Chem.* **2015**, *2015*, 1226–1232.
- [4] X. Bu, Y. Zhou, C. Li, F. Huang, *J. Appl. Polym. Sci.* **2016**, *133*, 3–9.
- [5] C. S. Hartley, *Nat. Chem.* **2014**, *6*, 91–92.
- [6] G. Bellussi, A. Carati, C. Rizzo, R. Millini, *Catal. Sci. Technol.* **2013**, *3*, 833–857.
- [7] K. Kawahara, H. Tachibana, Y. Hagiwara, K. Kuroda, *New J. Chem.* **2012**, *36*, 1210.
- [8] K. Kawahara, Y. Hagiwara, K. Kuroda, *Chem. Eur. J.* **2011**, *17*, 13188–13196.
- [9] Y. Hagiwara, A. Shimojima, K. Kuroda, *Chem. Mater.* **2008**, *20*, 1147–1153.
- [10] A. Shimojima, R. Goto, N. Atsumi, K. Kuroda, *Chem. Eur. J.* **2008**, *14*, 8500–8506.
- [11] S. Zhang, *Mater. Today* **2003**, *6*, 20–27.
- [12] I. Hasegawa, K. Hibino, K. Takei, *Appl. Organomet. Chem.* **1999**, *13*, 549–554.
- [13] J. Matison, C. Hartmann-Thompson, in *Advances in Silicon Science* Springer **2011**.

- [14] T. A. Tereshchenko, *J. Polym. Sci. Part B* **2008**, *50*, 249–262.
- [15] D. B. Cordes, P. D. Lickiss, F. Rataboul, *Chem. Rev.* **2010**, *110*, 2081–2173.
- [16] D. Gnanasekaran, K. Madhavan, B. S. R. Reddy, *J. Sci. Ind. Res.* **2009**, *68*, 437–464.
- [17] C. Baelocher, L. B. Mccusker, D. H. Olson, *Atlas of Zeolite Framework Types*, 6th edn., **2007**.
- [18] H. Gerke, H. Gies, F. Liebau, in *Soluble Silicates*, American Chemical Society Symposium Series **1982**, pp. 305–318.
- [19] Y. F. Shepelev, Y. I. Smolin, A. Ershov, O. Rademacher, H. Scheler, *Kristallografiya* **1987**, *32*, 1399–1403.
- [20] M. Wiebcke, D. Hoebbel, *J. Chem. Soc. Dalton Trans.* **1992**, 2451.
- [21] P. L. H. Verlooy, K. Robeyns, L. Van Meervelt, O. I. Lebedev, G. Van Tendeloo, J. A. Martens, C. E. A. Kirschhock, *Microporous Mesoporous Mater.* **2010**, *130*, 14–20.
- [22] I. Hasegawa, K. Ino, H. Ohnishi, *Appl. Organomet. Chem.* **2003**, *17*, 287–290.
- [23] H. Liu, S. I. Kondo, N. Takeda, M. Unno, *J. Am. Chem. Soc.* **2008**, *130*, 10074–10075.
- [24] K. Szubert, B. Marciniak, M. Dutkiewicz, M. J. Potrzebowski, H. Maciejewski, *J. Mol. Catal. A* **2014**, *391*, 150–157.
- [25] M. Dutkiewicz, M. Szołyga, H. Maciejewski, B. Marciniak, *J. Therm. Anal. Calorim.* **2014**, *117*, 259–264.
- [26] Y. Zhou, X. Bu, F. Huang, L. Du, G. Liang, *J. Wuhan Univ. Technol. Mater. Sci. Ed.* **2015**, *30*, 1310–1316.
- [27] D. Holzinger, G. Kickelbick, *J. Polym. Sci. Part A* **2002**, *40*, 3858–3872.
- [28] M. Barczewski, M. Dobrzyńska-Mizera, M. Dutkiewicz, M. Szołyga, *Polym. Int.* <https://doi.org/10.1002/pi.5158>.
- [29] P. A. Agaskar, *J. Am. Chem. Soc.* **1989**, *111*, 6858–6859.
- [30] G. Hayase, K. Kanamori, M. Fukuchi, H. Kaji, K. Nakanishi, *Angew. Chem. Int. Ed.* **2013**, *52*, 1986–1989; *Angew. Chem.* **2013**, *125*, 2040–2043.
- [31] C. Zhang, F. Babonneau, C. Bonhomme, R. M. Laine, C. L. Soles, H. A. Hristov, A. F. Yee, *J. Am. Chem. Soc.* **1998**, *120*, 8380–8391.
- [32] Y. Hagiwara, A. Shimojima, K. Kuroda, *Bull. Chem. Soc. Jpn.* **2010**, *83*, 424–430.
- [33] D. R. Do Carmo, L. S. Guinesi, N. L. Dias Filho, N. R. Stradiotto, *Appl. Surf. Sci.* **2004**, *235*, 449–459.
- [34] E. L. Heeley, D. J. Hughes, P. G. Taylor, A. R. Bassindale, *RSC Adv.* **2015**, *5*, 34709–34719.
- [35] N. Auner, B. Ziemer, B. Herrschaft, W. Ziche, P. John, J. Weis, *Eur. J. Inorg. Chem.* **1999**, *49*, 1087–1094.
- [36] R. M. Laine, *J. Mater. Chem.* **2005**, *15*, 3725–3744.
- [37] U. S. patent 7, 576,169, **2009**.
- [38] M. Wiebcke, M. Grube, H. Koller, G. Engelhardt, J. Felsche, *Microporous Mater.* **1993**, *2*, 55–63.
- [39] R. K. Harris, B. E. Mann, *NMR and the periodic table*, Academic Press **1978**.
- [40] S. D. Kinrade, C. T. G. Knight, D. L. Pole, R. T. Syvitski, *Inorg. Chem.* **1998**, *37*, 4278–4283.
- [41] M. J. Frisch, G. W. Trucks, H. B. Schlegel, G. E. Scuseria, M. A. Robb, J. R. Cheeseman, G. Scalmani, V. Barone, G. A. Petersson, H. Nakatsuji, X. Li, M. Caricato, A. Marenich, J. Bloino, B. G. Janesko, R. Gomperts, B. Menucci, H. P. Hratchian, J. V. Ortiz, A. F. Izmaylov, J. L. Sonnenberg, D. Williams-Young, F. Ding, F. Lipparini, F. Egidi, J. Goings, B. Peng, A. Petrone, T. Henderson, D. Ranasinghe, V. G. Zakrzewski, J. Gao, N. Rega, G. Zheng, W. Liang, M. Hada, M. Ehara, K. Toyota, R. Fukuda, J. Hasegawa, M. Ishida, T. Nakajima, Y. Honda, O. Kitao, H. Nakai, T. Vreven, K. Throssell, J. A. J. Montgomery, J. E. Peralta, F. Ogliaro, M. Bearpark, J. J. Heyd, E. Brothers, K. N. Kudin, V. N. Staroverov, T. Keith, R. Kobayashi, J. Normand, K. Raghavachari, A. Rendell, J. C. Burant, S. S. Iyengar, J. Tomasi, M. Cossi, J. M. Millam, M. Klene, C. Adamo, R. Cammi, J. W. Ochterski, R. L. Martin, K. Morokuma, O. Farkas, J. B. Foresman, D. J. Fox, *Gaussian 16, Revision D.01*, Gaussian Inc., Wallingford CT.
- [42] A. D. Becke, *J. Chem. Phys.* **1993**, *98*, 5648–5652.
- [43] S. Grimme, S. Ehrlich, L. Goerigk, *J. Comput. Chem.* **2011**, *32*, 1456–1465.
- [44] R. Krishnan, J. S. Binkley, R. Seeger, J. A. Pople, *J. Chem. Phys.* **1980**, *72*, 650–654.
- [45] a) D. McLean, G. S. Chandler, *J. Chem. Phys.* **1980**, *72*, 5639–5648.
- [46] J. P. Merrick, D. Moran, L. Radom, *J. Phys. Chem. A* **2007**, *111*, 11683–11700.
- [47] K. M. Delak, T. C. Farrar, N. Sahai, *J. Non-Cryst. Solids* **2005**, *351*, 2244–2250.
- [48] Q. Cheng, S. Debnath, E. Gregan, H. J. Byrne, *J. Phys. Chem. C* **2010**, *114*, 8821–8827.
- [49] P. Sen, K. Suresh, R. Vinoth Kumar, M. Kumar, G. Pugazhenthii, *J. Sci. Adv. Mater. Devices* **2016**, *1*, 311–323.
- [50] G. Kresse, J. Hafner, *Phys. Rev. B* **1993**, *48*, 13115–13118.
- [51] J. P. Perdew, K. Burke, M. Ernzerhof, *Phys. Rev. Lett.* **1996**, *77*, 3865–3868.
- [52] M. de Jong, W. Chen, T. Angsten, A. Jain, R. Notestine, A. Gamst, M. Sluiter, C. Krishna Ande, S. van der Zwaag, J. J. Plata, C. Toher, S. Curtarolo, G. Ceder, K. A. Persson, M. Asta, *Sci. Data* **2015**, *2*, 150009.
- [53] G. Gatta, Y. Lee, *Mineral. Mag.* **2014**, *78*, 267–291.
- [54] D. Fuard, T. Tzvetkova-Chevolleau, S. Decossas, P. Tracqui, P. Schiavone, *Microelectron. Eng.* **2008**, *85*, 1289–1293.
- [55] R. W. Warfield, F. R. Barnet in *Elastic Constants of Bulk Polymer* **1972**.
- [56] E. Rochow, *An Introduction Chemistry Of The Silicones*, John Wiley And Sons Inc. **1946**.
- [57] J. F. Brown, L. H. Vogt, A. Katchman, J. W. Eustance, K. M. Kiser, K. W. Krantz, *J. Am. Chem. Soc.* **1960**, *82*, 6194–6195.
- [58] D. H. Flagg, T. J. McCarthy, *Macromolecules* **2016**, *49*, 8581–8592.
- [59] S. G. Vasil'ev, V. I. Volkov, E. A. Tatarinova, A. M. Muzafarov, *Appl. Magn. Reson.* **2013**, *44*, 1015–1025.
- [60] S. G. Vasil'ev, V. I. Volkov, E. A. Tatarinova, A. M. Muzafarov, *Appl. Magn. Reson.* **2014**, *45*, 315–328.
- [61] Z. Yuan, J. Wang, *J. Elastomers Plast.* **2017**, *49*, 157–172.
- [62] I. Blanco, L. Abate, F. A. Bottino, P. Bottino, *J. Therm. Anal. Calorim.* **2014**, *117*, 243–250.
- [63] E. Verheyen, L. Joos, K. Van Havenbergh, E. Breynaert, N. Kasian, E. Go-bechiya, K. Houthoofd, C. Martineau, M. Hinterstein, F. Taulelle, V. Van Speybroeck, M. Waroquier, S. Bals, G. Van Tendeloo, C. E. A. Kirschhock, J. A. Martens, *Nat. Mater.* **2012**, *11*, 1059–1064.

Manuscript received: March 20, 2017

Accepted manuscript online: June 7, 2017

Version of record online: July 17, 2017